Materials Sciences and Applications, 2011, 2, 1631-1638
doi:10.4236/msa.2011.211217 Published Online November 2011 (http://www.SciRP.org/journal/msa)

Photoelectrochemical Production of Hydrogen in Aqueous Suspensions Nanoparticles Composites of CdS/ZnS

Kasem K. Kasem*, Melissa Dahn, Nida Zia, Aubrey Finney

Science, Mathematics & Information Department, School of Arts & Science, Indiana University Kokomo, Kokomo, USA.
Email: *kkasem@iuk.edu

Received July 20th, 2011; revised September 2nd, 2011; accepted September 19th, 2011.

ABSTRACT

Aqueous solutions of mixed CdS/ZnS semiconductor (*SC*) *nanoparticle suspensions in phosphate buffers containing* 10 *mM* $[Fe(CN)_6]^{4-}$ *were used for photochemical production of hydrogen via hydrated electron intermediates. CdS was doped with varying percentages of ZnS to expand the absorption range of the composite to the UV region. Results show that maximum generation of hydrated electrons by* $[Fe(CN)_6]^{4-}$ *occurs at pH* 6. *Furthermore, native CdS amorphous nanoparticles give the greatest photocurrent. Studies also show that, in phosphate buffer, the steady state photocurrent was directly proportional to the CdS content in the mixture of CdS/ZnS. The aqueous nano-systems sustained their stability as indicated by the reproducibility of their photocatalytic activities. Solar radiated assemblies of CdS/ZnS/* $[Fe(CN)_6]^{4-}$ *sustained cyclic systems for continuous hydrogen production.*

***Keywords*:** *Photolysis*, *Nanoparticles*, *Hydrogen*, *Suspensions*, *Cadmium Sulfide*

1. Introduction

Traditional chemical or electrochemical methods for production of hydrogen tend to be complicated and energy consuming process. Some of these methods are not even environmentally safe. Novel methods that avoidthe disadvantages of traditional methods are in demand. The use of solar radiation in photolysis of water, can be one of these novel methods that can meet this demand. Evidences that some semiconductors (SC) mediate hydrogen production during photolysis of water werereported by several researchers [1-8]. Nano-sized metal chalcogenides such as sulfides, selenides, and tellurides with a specific band gap that can serve this purpose are being produced following a variety of procedures [9-14]. The photocurrent obtained using such nano-sized assemblies is often low because fast charge recombination limits photocurrent generation. When composite semiconductors are used it is possible to improve the efficiency of charge separation through charge rectification. This can take place by modifying either the surface of the base semiconductor or its composition with inorganic or organic semiconductors.

In some studies [11] nano-size semiconductors were used because of their larger surface area and their ability to carry out all the reactions that were previously associated with thin solid films of semiconductor electrodes. TiO_2 (Titania) is known as a photo catalysis agent for a wide range of substances [15]. Nano-sized TiO_2 possesses enhanced photocatalytic activity and solar energy conversion [16,17]. However, some disadvantages limit the efficient use of TiO_2. For example, the high band gap energy (3.2 eV) of TiO_2 requires UV radiation for photoactivation, limiting its application in the visible light range, and charge carrier recombination (e^-/h^+) occurs within nanoseconds, limiting its photocatalytic activity [18]. The spatial separation between oxidative and reductive sites is very small and increases the occurrence of back reactions.

CdS has been intensively studied [19-23] due to advantages such as its band-gap energy in the visible region Eg = 2.5 eV and its relatively simple fabrication process. CdS nano-particles often present novel properties and have been widely used in solar cells [24], optoelectronics, and microelectronics. CdS particles form a group of direct band gap materials suitable for light emitting applications, and their luminescent properties have been studied extensively [25]. The small size of nanoparticles leads to their larger surface area, which will increase the

number of surface specific active sites for both chemical reactions and photon absorption. When particle size decreases below the Bohr radius of the first excitation state, quantum size effects can occur due to the confinement of charge carriers [26].

Although the stability conditions are not met by CdS because its decomposition potential ($E_{p,d}$) is less than the oxidation potential of water (E_{O_2/H_2O}), its reduction potential is more negative than that of H^+. Mixing CdS and ZnS by co-deposition may push the limits of the CdS/ZnS band structure to the level where the decomposition potential is greater than that the decomposition of water.

Effective conversion of solar energy to chemical energy in hydrogen form, requires an inexpensive source that contains hydrogen and has a large surface area. Aqueous colloidal nanoparticle suspensions meet these requirements. The suspension media are equally as important as the suspension particles in generating an efficient photolysis process. Previous studies used semiconductor particles as photoactive systems in heterogeneous charge transfer processes at the particle/electrolyte interface [27, 28]. Hydrated electrons can play an important role in photo-dissociation of water through this reaction:

$$[Fe(CN)_6]^{4-} + \mathbf{h\nu} = [Fe(CN)_6]^{3-} + e_{aq} \quad (1)$$

$$e_{aq} + e_{aq} = H_2 + 2OH^- \quad (2)$$

($aq^- = H_2O$)

$$2[Fe(CN)_6]^{4-} + 2\mathbf{h\nu} = 2[Fe(CN)_6]^{3-} + H_2 + 2OH^- \quad (3)$$

The molecular orbital structure of hexacyano iron (II), $[Fe(CN)_6]^{4-}$, allows electronic transitions under the photo excitation condition and produces hydrated electrons that react according to the above reaction. $[Fe(CN)_6]^{4-}$ undergoes oxidation to $[Fe(CN)_6]^{3-}$. The disadvantage of a homogeneous process for hydrated electron production is its irreversibility. However, such a disadvantage can be overcome by the use of a semiconductor system which acts as an electron donor and reduces $[Fe(CN)_6]^{3-}$ back to $[Fe(CN)_6]^{4-}$. Achieving such a goal will create the conditions of reversible ergo-dynamics.

A means to expand CdS band gap for efficient capture of UV-visible radiation is mixing it with ZnS which possesses a greater band gap than CdS.

In this paper we investigated the effect of alteringthe band gap of the mixed CdS/ZnS composite by changing the percentage of ZnS on the photocatalytic behavior of composite suspensions in buffered ferrocyanide solutions as the hydrated electron supplier. Conditions that maximize the production of hydrated electrons were also explored.

2. Experimental

Reagents: All reagents were of analytical grade. All solutions were prepared using de-ionized water, unless otherwise stated. CdS/ZnS composites were prepared as described elsewhere [29].

Instrumentation: All electrochemical experiments were carried out using a conventional three-electrode cell consisting of Pt wire as a counter electrode, Ag/AgCl as a reference electrode, and Pt gauze as an electron collector. A BAS 100 W electrochemical analyzer (Bio-analytical Co.) was used to perform the electrochemical studies. Steady state reflectance spectra were recorded using a Shimadzu UV-2101 PC. Branson Model 250 digital sonifier was used to break down powder to the desired nano-particle size.

Sample preparation: The colloidal nano-particle suspensions were prepared by dispersing 50 mg of the semiconductors powder in 100 mL of the bufferusing high energy sonicators. Preliminary studies with large particle sizes (500 - 1000 nm) gave poor photo responses. We did our studies on diverse collections of small-particles sizes blow 200 nm. An Olympus BX-FLA60 reflected light fluorescence microscope using polarized light at a wavelength range between 330 to 550 nm was used to make sure that the size of the suspensions of colloidal nanoparticles did not exceed 200 nm.

Photolysis cell: The electrolysis cell was a one compartment 120 mL Pyrex cell with a quartz window facing the irradiation source. A 10-cm^2 platinum gauze cylinder was used as working electrode. Aqueous suspensions were stirred with a magnetic stirrer during the measurements. An $Ag/AgCl/Cl^-$ reference electrode was also fitted into this compartment. A 10-cm^2 platinum counter electrode was housed in a glass cylinder sealed at one end with a fine porosity glass frit. The pH was adjusted by addition of either 1 M NaOH or 1 M H_3PO_4.

Irradiations were performed with a solar simulator 300 watt xenon lamp (Newport) with an IR filter. Light was focused on the cell window using a metal cylinder with 5 cm diameter, and 15 cm length. The cell position was adjusted to allow full illumination of the 100 mL suspension. Photolysis of $[Fe(CN)_6]^{4-}$ generated hydrated electrons and $[Fe(CN)_6]^{3-}$. The potential of the working electrode was fixed at 100 mV more negative than the reduction potential of $[Fe(CN)_6]^{3-}$ to guarantee full reduction of ferricyanide. The current due to the reduction of $[Fe(CN)_6]^{3-}$ collected by the working electrode during the photolysis process was a measure of photocurrent. Photocurrent-time curves were obtained with a BAS 100 W Bioanalytical system. The measured photocurrent was normalized to $A \cdot m^{-2} \cdot h^{-1}$ (ampere per square meter per hour) of illumination. Because the measured photocurrent is a function of regeneration of ferrocyanide (the solvated electron suppliers that generate hydrogen), the measured photocurrent was normalized considering two photons per one hydrogen molecule (according to Equa-

tion (2)), and was used to calculate the number of moles of hydrogen generated per square meter per hour of illumination. Hydrogen was detected using HY-ALERTA™ 500 (h2 scan California).

The following equation was used to calculate H_2 rate:

$$\mathrm{H_2rate}\left(\mathrm{mole}\cdot\mathrm{m}^{-2}\cdot\mathrm{h}^{-1}\right) = \frac{i\left(c*\mathrm{mole}^{-1}\right)*10^4\left(\mathrm{cm}^2\right)*3.6*10^3\mathrm{s}}{2*96500\left(c*\mathrm{mole}^{-1}*a\left(\mathrm{cm}^2\right)\right)} \quad (4)$$

where i = photo current, C/s., a = electrode surface area, cm^2, 3600 s corresponds to one hour, 10,000 corresponding to one square meter, and 96,500 C/mole corresponds to the Farad.

3. Results and Discussion

3.1. Energy Map of CdS/ZnS Composite

Figure 1 illustrates the diffusive reflectance absorption spectra of CdS/ZnS nanoparticle composites. Determination of direct and indirect band gap of the studied mixtures was done using the following Tauc equations [30]:

$$\left(\alpha E_\gamma\right)^2 \propto E_\gamma - E_{gd} \quad (5)$$

$$\alpha \propto \frac{\left(E_\gamma + E_p - E_{gi}\right)^2}{e^{\left(E_\gamma/(kT)\right)}-1} + \frac{\left(E_\gamma + E_p - E_{gi}\right)^2 e^{\left(E_\gamma/(kT)\right)}}{e^{\left(E_\gamma/(kT)\right)}-1} \quad (6)$$

where α is an absorption coefficient, and E_g is the optical band gap. Analysis of the data provided by **Figure 1**, indicates that the studied CdS/ZnS mixtures possess a direct and indirect band gap. **Figure 2** shows that these band gaps varied monotonically with the percent composition between that of ZnS and the smaller band gap of CdS. The fact that the absorption of the mixture underwent blue shift, indicates that the band gap of the mixture is being expanded to absorbshorter wave length. The relative location of the C.B (conduction band) of CdS as

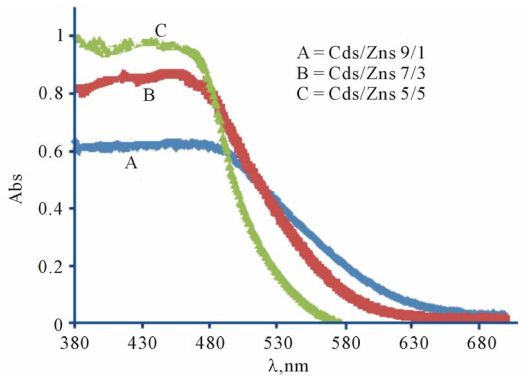

Figure 1. Steady state reflectance spectra for CdS/ZnS Composites. Inset SEM for the CdS/ZnS particles before sonication.

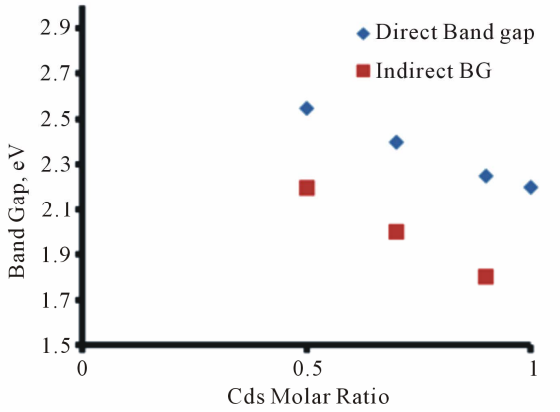

Figure 2. Changes in the direct and indirect band gap with ZnS percentage in the composites.

a major compound in the mixture is about –0.4 V vs NHE, which is more negative to the redox potential of $[Fe(CN)_6]^{4-/3-}$ than the reduction potential of H^+. This guarantees the reduction of $[Fe(CN)_6]^{3-}$. The band gap of the mixture increases by increasing the percentage of ZnS due to the fact that ZnS possesses a greater band gap than CdS. The intensity of UV in the used solar simulator is much less than that of VIS portion. Addition of ZnS makes the mixture less efficient in the absorption of the VIS light. The observed photochemical outcome and consequently, hydrogen production of the prepared mixtures (premonition) decreases by increasing ZnS in the mixture. This makes the data for indirect band gap displayed in **Figure 2** irrelevant. This is because the indirect band gap of samples with greatest content of ZnS (50%) is less than 2.3 eV (smaller than that of pure CdS). We concluded that the samples used in this study acted with direct band gap transitions. These studied nano particles give similar photocurrent in aerated and de aerated buffers containing $[Fe(CN)_6]^{4-}$. These results show no effect of de-aeration process on the photolysis process. This also indicates that the C.B did not shift to more negative value (cathodically) to cover the reduction potential [31]of the dissolved oxygen (≈ –0.8 V vs NHE). Although increasing ZnS did not increase the direct band gap of the mixture with amount proportional to ZnS content (**Figure 2**), the decrease in photocurrent reflects that ZnS did not causes catholic shift for the flatband potential of CdS. These two observations support general conclusion that the addition of ZnS may cause an upward shift in the valence band.

3.2. Photolysis of Aqueous Solutions of $[Fe(CN)_6]^{4-}$ Effect of pH

One of the products of reaction 3 is OH^-, which makes this reaction pH dependant. This reaction product suggests that an acid pH range would be suitable to shift its

equilibrium to favor of H_2 production. However, $[Fe(CN)_6]^{4-}$ as a reactant is pH sensitive. We have found that, at pH less than 6, $[Fe(CN)_6]^{4-}$ will form a green compound known as Berlin green or ferric ferrocyanide $[Fe(CN)_6]^{3-}$. Photolysis reactions of aqueous $[Fe(CN)_6]^{4-}$ in phosphate buffer at different pH values were performed. The results are displayed in **Figure 3**, from which we can notice a drop in photocurrent at pH greater than 6. For these reasons, photolysis of aqueous $[Fe(CN)_6]^{4-}$ in the presence of CdS/ZnS mixture nano- particles took place at pH 6. The observed change shown in **Figure 3** can be attributed to the kinetics of reduction of $[Fe(CN)_6]^{3-}$ on the Pt electrode and the presence of some Pt oxides formed at pH greater than 6 as indicated by Pourbaix diagrams [32]. The kinetics of such reductions at higher pH is beyond the scope of this article and it can be a subject of future studies.

3.3. Photolysis of Aqueous $[Fe(CN)_6]^{4-}$ in the Presence of CdS/ZnS Suspensions

Aqueous suspensions of pure CdS in 0.2 M phosphate buffer containing 10 mmole of $[Fe(CN)_6]^{4-}$ at pH 6 were subject to the photolysis process. The potential of the Pt collector electrode kept constant at 0.000 V vs Ag/AgCl. The results are displayed in **Figures 4** and **5**. The recorded photocurrent in **Figure 4** is due to electrochemical reduction of $[Fe(CN)_6]^{3-}$. In the presence of illuminated CdS, reduction of $[Fe(CN)_6]^{3-}$ can take place by an electrochemical and/or by a photochemical process. The collector electrode records only the electrochemical process. The amount of $[Fe(CN)_6]^{3-}$ reduced by the photochemical process can be estimated by the difference between the current recorded for the photolysis of $[Fe(CN)_6]^{4-}$ at pH 6 in the absence and in the presence of SC according to the following equation:

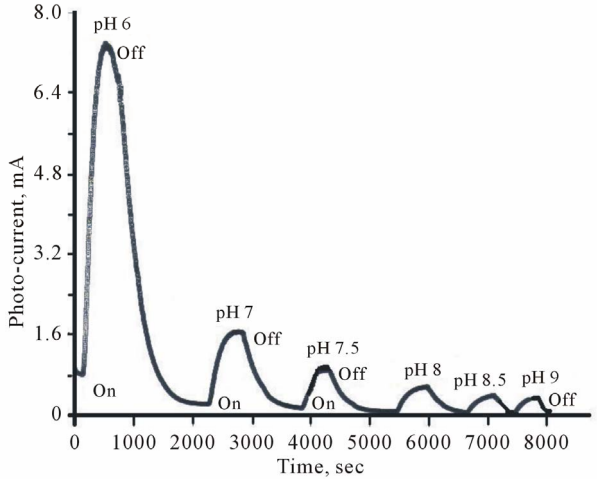

Figure 3. Effect of pH on the recorded photocurrent during the photolysis of $[Fe(CN)_6]^{4-}$.

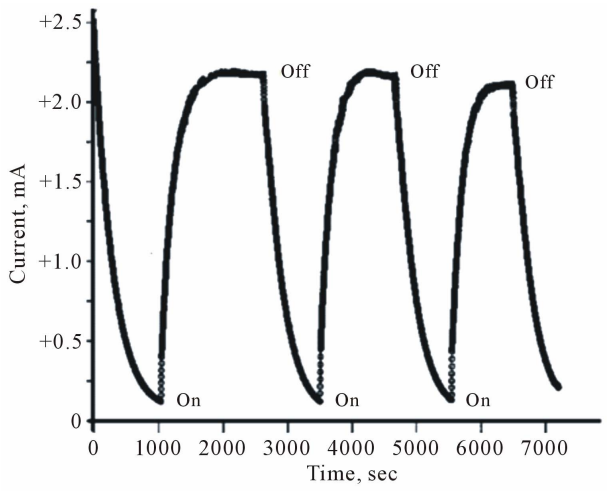

Figure 4. Reproducibility of the photocurrent during the photolysis of $[Fe(CN)_6]^{4-}$ in presence of pure CdS nanoparticle suspensions.

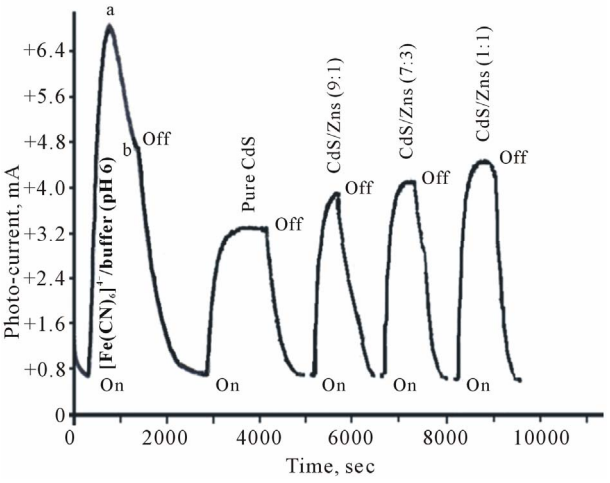

Figure 5. Photolysis of aqueous CdS/ZnS nanoparticles in 10 mM $[Fe(CN)_6]^{4-}$/Phosphate buffer (pH = 6).

Photo-reduction current $I_{photored} = I_{red}$ in absence of SC – I_{red} in presence of SC (7)

It can be noticed that the recorded I_{red} (Equation (7)) in the presence of SC (**Figures 4** and **5**) is less than that recorded for 10 mmole of $[Fe(CN)_6]^{4-}$ only (**Figure 3**). Furthermore, **Figure 4** indicates that the recorded current is reproducible at almost constant valuesindicating that CdS particles maintained their stability against photodeteriorations. It can be noticed also from **Figure 5**, that the steady state current (point a) for the reference (10 mmole of $[Fe(CN)_6]^{4-}$ at pH 6) has very small plateau (ca 120 s) and is followed by a gradual decrease in the recorded current under dark condition (point b) while, in the presence of CdS (**Figure 4**), the plateau of the peak current is large (ca 1000 s), followed by a sharp drop

under dark conditions. Such a large steady state current plateau is an enhancing factor in photolysis processes in suspension systems. The slope of line ab in **Figure 5** is smaller than the slope of line bc. This can be attributed to the slow diffusion of $[Fe(CN)_6]^{3-}$ to the collector electrode.

The drop in the reduction current for the reference system even under illumination can be explained by the fact that at steady state peak current, the high concentration of $[Fe(CN)_6]^{4-}$ captivated by the cylindrical mesh of the Pt electrode creates a local concentration overvoltage. This overvoltage reduces the diffusion of $[Fe(CN)_6]^{3-}$ formed in the bulk electrolyte. Under dark conditions no more $[Fe(CN)_6]^{3-}$ is formed and the reduction of remaining $[Fe(CN)_6]^{3-}$ is irreversible. This causes the greater drop along the line bc. Similar reasoning can be used to explain the observed results obtained for CdS/ZnS mixtures displayed in **Figure 5**. The larger plateau observed with this suspension than with the reference sample indicates that the suspension particles adsorb the reduction product, eliminating the concentration overvoltage. This allows a steady amount of $[Fe(CN)_6]^{3-}$ to reach the collector electrode. **Figure 5** also indicates that as the ZnS percentage increases, the photo-reduction current (Equation (5)) decreases. When pure ZnS nanoparticles were used the measured photo-reduction current was the least as shown in **Figure 6**.

3.4. Photolysis of Aqueous Solutions of $[Fe(CN)_6]^{4-}$ in Basic Media

Working at pH 9 using platinum as collector electrode requires a potential of less than 0.4 V vs NHE, or 0.2 V vs Ag/AgCl. The kinetics of reduction of $[Fe(CN)_6]^{3-}$ are slow at pH 9 as indicated by **Figure 3**. The reduction currents reported for $[Fe(CN)_6]^{3-}$ in the presence of the studied suspensions at pH 9 were greater than those reported in absence of these suspensions indicating that more $[Fe(CN)_6]^{3-}$ is produced in the presence of CdS/ZnS mixtures through oxidation of $[Fe(CN)_6]^{4-}$.

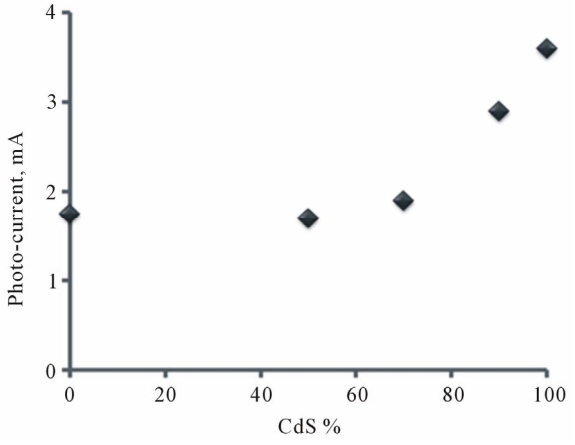

Figure 6. Effect of CdS percentage on the photocurrent during the photolysis of $[Fe(CN)_6]^{4-}$ in presence of CdS/ZnS nanoparticle suspensions.

Such results can be explained on the basis that the CdS /ZnS particles acted as a n-type semiconductor at pH 9, and the following reaction took place

$$2\left[Fe(CN)_6\right]^{4-} + 2\mathbf{hv} + \bullet(e/h) = 2\left[Fe(CN)_6\right]^{3-} + e_{aq} + H\,(atthe\ \text{C.B}) \quad (8)$$

(The dot●, in equation 8, represent the nanoparticles of CdS or CdS/ZnS). In reaction 8 formation of $[Fe(CN)_6]^{3-}$ is due to the action of both the direct light oxidation of $[Fe(CN)_6]^{4-}$ and the oxidation of n-type nanoparticles. Because we focused our studies on homogeneous production of hydrogen, the amount of hydrogen formed at the C.B was not measured and therefore was not included in the obtained results.

Because the Pt electrode was potentiosated at 0.00 V vs Ag/AgCl (0.2 V vs NHE), the collector electrode maintained it immunity against corrosion [31,32]. Therefore the increase of the reduction current is due to a photolysis process rather than a catalytic process that can take place if PtO_2 existed [32]. This also would reflect the dual nature of nanoparticle suspensions. Upon illumination, reactions 1 and 3 take place simultaneously. According to reaction 3, at pH 9 $[Fe(CN)_6]^{4-}$ acted as hole scavenger and oxidized to $[Fe(CN)_6]^{3-}$. This increased the amount of $[Fe(CN)_6]^{3-}$ reduced electrochemically.

3.5. Hydrogen Production in the Photolysis Process

The results displayed in **Figures 3**, **4**, and **5** indicate that $[Fe(CN)_6]^{4-}$ is an excellent supplier of hydrated electrons that produce hydrogen according to reaction 3. The continuous presence of $[Fe(CN)_6]^{4-}$ will insure the generation of hydrated electrons and, consequently, hydrogen. Rates of hydrogen production via regeneration of $[Fe(CN)_6]^{4-}$ by photochemical reduction of $[Fe(CN)_6]^{3-}$ at semiconductor surfaces are listed in **Table 1**. The data listed in this table indicate that pure CdS generated hydrogen at the greatest rate among the studied mixtures. As the percentage of ZnS increases, the rate of hydrogen production decreases. On the other hand, rates of hydrogen production via regeneration of $[Fe(CN)_6]^{4-}$ by electrochemical reduction of $[Fe(CN)_6]^{3-}$ at a Pt electrode are displayed in **Figure 7**. Contrary to the results listed in **Table 1**, **Figure 6** indicates that, as the percentage of ZnS in the mixture increases, the hydrogen production rate increases. This observation is consistent with fact that $Fe(CN)_6]^{3-}$ is reduced by photolysis and electro chemical

Table 1. Hydrogen production rate during the photolysis process of $[Fe(CN)_6]^{4-}$ in the aqueous suspensions of the studied nanoparticles.

Semiconductor compostion (mass percent)	Steady state H_2 production, mole·h^{-1}·m^{-2}
CdS 100%	0.0676
CdS/ZnS 90:10	0.0546
CdS/ZnS 70:30	0.0341
CdS/ZnS 50:50	0.0316

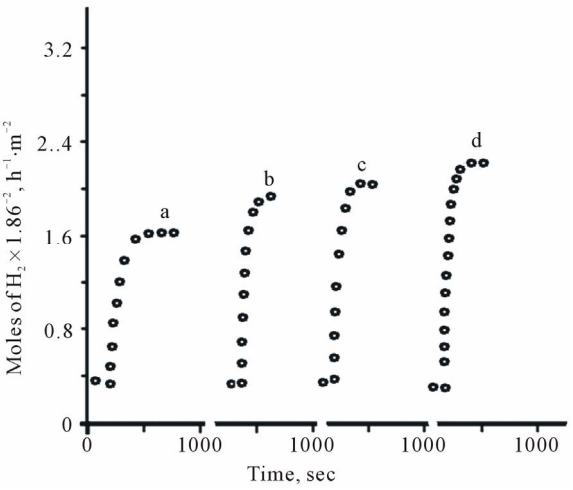

Figure 7. H_2 prodiced via electrochemical redcution of $[Fe(CN)_6]^{4-}$ in phospahe buffer at pH 6, in presence of (a) CdS; (b) CdS/ZnS (9:1); (c) CdS/ZnS (7:3); (d) CdS/nS (5:5).

processes. Electrochemical reduction occurs very readily in presence of high percentages of ZnS. Reduction in the presence of substances with no or low concentrations of ZnS occur primarily through a photochemical process. Because the amount of $[Fe(CN)_6]^{3-}$ generated in reaction 3 is constant, when the product of one process increases, the product of the other process decreases.

4. Conclusions

The low band gap of CdS (2.3 eV) generated the greatest photochemical production of hydrogen compared with its mixtures with ZnS. This indicates that the addition of ZnS widened the band gap of the CdS/ZnS alloy, resulting in less absorption of the solar radiation. This widening of the band gap took place by a downward shift of the valence band, and asmall upward shift in the conduction band of the CdS/ZnS alloy.Studies show that the direct band gap of mixed CdS/ZnS materials varied monotonically with the percent of CdS in the mixture. Photonic transitions that cause the photolysis process occurred mainly by the direct band transition [33]. Maximum photochemical response during the photolysis of $[Fe(CN)_6]^{4-}$ was reported at pH 6. The amount of $[Fe(CN)_6]^{3-}$ reduced via the photochemical process decreased by increasing ZnS content in the mixture (**Figure 6**). The reproducibility of thephotocatalytic activities of CdS/ZnS nanoparticles is an indication that these systems sustained their stability under illumination conditions. The problems related to heterogeneous production of hydrogen were eliminated, as hydrogen was generated via homogenous photoreaction in these heterogeneous suspensions. This process can be scaled up for large scale hydrogen production. Using such a method in industry makes the production process of hydrogen totally green. This is because the homogenous production of hydrogen by photolysis and heterogonous reduction of $[Fe(CN)_6]^{3-}$ to generate $[Fe(CN)_6]^{4-}$ can take place by solar energy powered potentiosate.

REFERENCES

[1] Y. J. Zhang, W. Yan, Y. P. Wu and Z. H. Wang, "Synthesis of TiO_2 Nanotubes Coupled with CdS.," *Materials Letters*, Vol. 62, No. 23, 2008, pp. 3846-3848. doi:10.1016/j.matlet.2008.04.084

[2] P. L. Gentili, M. Penconi, F. Ortica, F. Cotana, F. Rossis and F. Elisei, "Synergistic Effects in Hydrogen Production through Water Sonophotolysis Catalyzed by New $La_{2x}Ga_{2y}In_{2(1-x-y)}O_3$ Solid Solutions," *International Journal of Hydrogen Energy*, Vol. 34, No. 22, 2009, pp. 9042-9049. doi:10.1016/j.ijhydene.2009.09.027

[3] K. Maeda, K. Teramura, D. Lu, N. Saito, Y. Inoue and K. Domen, "Noble-Metal/Cr_2O_3 Core/Shell Nanoparticle as a Cocatalyst," *Angewandte Chemie*, *International Edition*, Vol. 45, No. 6, 2006, pp. 7806-7809. doi:10.1002/anie.200602473

[4] T. Lindgren, L. Vayssieres, H. Wang and S. E. Lindquist, "The Emergence of a New Generation of Smart Materials," *Chemical Physics of Nanostructured Semiconductors*, Vol. 83, 2003, pp. 110-116.

[5] J. S. Jang, H. G. Kim, V. R. Reddy, S. W. Bae, S. M. Ji and J. S. Lee, "Highly Donor-Doped (110) Layered Perovskite as Novel Photocatalysts," *Journal of Catalysis*, Vol. 231, No. 1, 2005, pp. 213-222. doi:10.1016/j.jcat.2005.01.026

[6] C. Huang, C. A. Linkous, O. Adebiyi and A. T-Raissi, "Hydrogen Production via Photolytic Oxidation of Aqueous Sodium Sulfite Solutions," *Environmental Science & Technology*, Vol. 44, No. 13, 2010, pp. 5283-5288. doi:10.1021/es903766w

[7] J. A. Villoria, Y. Navarro, M. Rufino, S. M. Al-Zahrani and J. L. G. Fierro, "Photocatalytic Hydrogen Production on Cd1-xZnxS Solid Solutions under Visible Light: Influence of Thermal Treatment," *Industrial & Engineering Chemistry Research*, Vol. 49, No. 15, 2010, pp. 6854-6861. doi:10.1021/ie901718r

[8] C. J. Sartoretti, B. D. Alexander, R. Slarska, I. A. Rut-

kowska, J. Augustynski and R. Cerny, "Photoelectrochemical Oxidation of Water at Transparent Ferric Oxide Film Electrodes," *The Journal of Physical Chemistry*, *B*, Vol. 109, No. 28, 2005, pp. 13685-13692. doi:10.1021/jp051546g

[9] C. J. Sartoretti, M. Ulmann, B. D. Alexander and B. D. Augustynski, "Nanostructured α-Fe_2O_3 Electrodes for Solar Driven Water Splitting," *The Journal of Chemical Physics Letters*, Vol. 376, 2003, pp. 194-200.

[10] L. M. Peter, K. G. U. Wijayantha, D. J. Riley and J. P. Waggett, "Band-Edge Tuning in Self-Assembled Layers of Bi_2S_3 Nanoparticles Used to Photosensitize Nanocrystalline TiO_2," *Journal of Physical Chemistry B*, Vol. 107, No. 33, 2003, pp. 8378-8381. doi:10.1021/jp030334l

[11] R. Vogel, P. Hoyer and H. Weller, "Quantum-Sized PbS, CdS, AgzS, Sb&, and Bi& Partic as Sensitizers for Various Nanoporous. Wide-Bandgap Semiconductors," *The Journal of Physical Chemistry*, Vol. 98, 1994, pp. 3183-3188. doi:10.1021/j100063a022

[12] R. Plass, S. Pelet, J. Krueger, M. Gratzel and U. Bach, "Quantum Dots Sensitization of Organic/Inorganic Hybrid Solar Cells," *Journal of Physical Chemistry B*, Vol. 106, No. 31, 2002, pp. 7578-7580. doi:10.1021/jp020453l

[13] K. Park, H. J. Yu, W. K. Chung, B.-J. Kim and S. H. Kim, "Effect of Heat-Treatment on CdS and CdS/ZnS Nanoparticles," *Journal of Materials Science*, Vol. 44, No. 16, 2009, pp. 4315-4320. doi:10.1007/s10853-009-3641-2

[14] D. Liu and P. V. Kamat, "Photoelectrochemical Behavior of Thin Cadmium Selenide Semiconductor Films," *The Journal of Physical Chemistry*, Vol. 97, No. 41, 1993, pp. 10769-10773. doi:10.1021/j100143a041

[15] M. J. Chen; Y. W. Tang, B. H. Li and L. J. Luo, "Nanocrystalline CdS/ZnO Thin Films: Fabrication and Application to Solar Cells," *Journal of Nanoscience and Nanotechnology*, Vol. 9, No. 2, 2009, pp. 1505-1508. doi:10.1166/jnn.2009.C189

[16] T. Peng, D. Zhao, H. Song and C. Yan, "Preparation of Lanthana-Doped Titania Nanoparticles with Anatase Mesoporous Walls and High Photocatalytic Activity," *Journal of Molecular Catalysis A*: *Chemical*, Vol. 238, No. 1-2, 2005, pp. 119-122. doi:10.1016/j.molcata.2005.04.066

[17] D. L. Liao and B. Q. Liao, "Shape, Size and Photocatalytic Activity Control of TiO_2 Nanoparticles with Surfactants," *Journal of Photochemistry and Photobiology*, *A*: *Chemistry*, Vol. 87, No. 2-3, 2007, pp. 363-369. doi:10.1016/j.jphotochem.2006.11.003

[18] C. C. Trapalis, P. Keivanidis, G. Kordas, M. Zaharescu, M. Crisan, A. Szatvanyi and M. Gartner, "$TiO_2(Fe^{3+})$ Nanostructured Thin Films with Antibacterial Properties," *Thin Solid Films*, Vol. 433, No. 1-2, 2003, pp. 186-190. doi:10.1016/S0040-6090(03)00331-6

[19] X. X. Yan, G. Liu, L. Z. Wang, Y. Wang, X. F. Zhu, J. Zou and G. Q. Lu, "Antiphotocorrosivephotocatalysts Containing CdS Nanoparticles and Exfoliated TiO_2 Nanosheets," *Journal of Materials Research*, Vol. 25, No. 1, 2010, pp. 182-188. doi:10.1557/JMR.2010.0007

[20] D. Dung, J. Ramsden and M. Graetzel, "Dynamics of Interfacial Electron-Transfer Processes in Colloidal Semi Conductor Systems," *Journal of the American Chemical Society*, Vol. 104, No. 11, 1982, pp. 2977-2985. doi:10.1021/ja00375a006

[21] M. AshaJhonsi, A. Kathiravan and R. Renganathan, "Photoinduced Interaction between Xanthene Dyes and Colloidal CdS Nanoparticles," *Journal of Molecular Structure*, Vol. 921, No. 1-3, 2009, pp. 279-284. doi:10.1016/j.molstruc.2009.01.006

[22] S. Drouard, S. G. Hickey and R. D. Jason, "CdS Nanoparticle-Modified Electrodes for Photoelectrochemical Studies," *Chemical Communications*, No. 1, 1999, pp. 67-68. doi:10.1039/a808572b

[23] S. G. Hickey and D. J. Riley, "Photoelectrochemical Studies of CdS Nanoparticle-Modified Electrodes," *Journal of Physical Chemistry B*, Vol. 103, No. 22, 1999, pp. 4599-4602. doi:10.1021/jp990020r

[24] H. Yildiz, R. Tel-Vered and I. Willner, "Solar Cells with Enhanced Photocurrent Efficiencies Using Oligoaniline-Crosslinked Au/CdS Nanoparticles Arrays on Electrodes," *Advanced Functional Materials*, Vol. 18, No. 21, 2008, pp. 3497-3505. doi:10.1002/adfm.200800810

[25] M. Saif and M. S. A. Abdel-Mottaleb, "Titanium Dioxide Nanomaterial Doped with Trivalent Lanthanide Ions of Tb, Eu and Sm: Preparation, Characterization and Potential Applications," *Inorganica Chimica Act*, Vol. 360, No. 9-10, 2007, pp. 2863-2874.

[26] S. A. Blanton, M. A. Hines and P. Guyot-Sionnest, "Photoluminescence Wandering in Single CdSe Nanocrystals," *Applied Physics Letters*, 1996, Vol. 69, No. 25, pp. 3905-3907.

[27] N. Serpone, D. Lawless and E. Pelizzetti, "Fine Particles Science and Technology," E. Pelizzetti, Ed., Kluwer Academics Publishers, New York, 1996, pp. 657-662.

[28] A. HaqueSaif, T. Park, A. B. Holmes and J. R. Durrant, "Transient Optical Studies of Interfacial Energetic Disorder at Nanostructured Dye-Sensitised Inorganic/Organic Semiconductor Heterojunctions," *Chemphyschem*: *A European Journal of Chemical Physics and Physical Chemistry*, Vol. 4, No. 1, 2003, pp. 89-93.

[29] S. Gordon, E. J. Hars, M. S. Matheson, J. Rahani and J. K. Thomas, "Reaction Constants of the Hydrated Electron," *Journal of American Chemical Society*, Vol. 85, No. 10, 1965, pp. 1375-1377. doi:10.1021/ja00893a002

[30] B. S. Amma, K. Manzoor, K. Ramakrishna and M. Pattabi, "Synthesis and Optical Properties of CdS/Zn Scoreshell Nanoparticles," *Materials Chemistry and Physics*, Vol. 112, No. 3, 2008, pp. 789-792. doi:10.1016/j.matchemphys.2008.06.043

[31] J. J. Van Benschoten. J. Y. Lewis, W. R. Heineman, D. A. Roston and P. T. Klsslnger, "Cyclic Voltammetry Experiment," *Journal of Chemical Education*, Vol. 60, No. 9, 1983, pp. 772-776. doi:10.1021/ed060p772

[32] M. Pourbaix, "Atlas of Electrochemical Equilibria in Aqueous Solutions," Pergamon Press, Brussels, 1966, pp. 359-363.

[33] L. G. Arriaga and A. M. Fernoandez, "Determination of Flat Band Potential and Photocurrent Response in (Cd,Zn)S Used in Photoelectrolysis Process," *International Journal of Hydrogen Energy*, Vol. 27, No. 1, 2002, pp. 27-31. doi:10.1016/S0360-3199(01)00084-2

